Phase-space Correlation in Stellar Streams of the Milky Way Halo: The Clash of Kshir and GD-1[*]

Khyati Malhan[1] ✦, Rodrigo A. Ibata[2] ✦, Raymond G. Carlberg[3] ✦, Michele Bellazzini[4] ✦, Benoit Famaey[2] ✦, and Nicolas F. Martin[2] ✦

[1] The Oskar Klein Centre for Cosmoparticle Physics, Department of Physics, Stockholm University, AlbaNova, SE-10691 Stockholm, Sweden
khyati.malhan@fysik.su.se
[2] Université de Strasbourg, CNRS, Observatoire Astronomique de Strasbourg, UMR 7550, F-67000 Strasbourg, France
[3] Department of Astronomy & Astrophysics, University of Toronto, Toronto, ON M5S 3H4, Canada
[4] INAF - Osservatorio di Astrofisica e Scienza dello Spazio, via Gobetti 93/3, I-40129 Bologna, Italy
Received 2019 August 29; revised 2019 October 30; accepted 2019 October 31; published 2019 November 14

Abstract

We report the discovery of a $70°$ long stellar stream in the Milky Way halo, which criss-crosses the well known "GD-1" stream. We show that this new stellar structure ("Kshir") and GD-1 lie at similar distance, and are remarkably correlated in kinematics. We propose several explanations for the nature of this new structure and its possible association with GD-1. However, a scenario in which these two streams were accreted onto the Milky Way within the same dark matter sub-halo seems to provide a natural explanation for their phase-space entanglement, and other complexities of this coupled system.

Unified Astronomy Thesaurus concepts: Globular star clusters (656); Dark matter (353); Stellar kinematics (1608); Milky Way stellar halo (1060)

1. Introduction

Stellar streams are "fossil" remnants of accretion events that are formed by the tidal disruption of satellite systems as they accrete and begin to orbit in the gravitational potential of the host galaxy. More than 50 streams have been detected so far in the Milky Way halo (e.g., Ibata et al. 2001; Belokurov et al. 2006; Grillmair 2009; Balbinot et al. 2016; Bernard et al. 2016; Myeong et al. 2017; Malhan et al. 2018; Shipp et al. 2018; Ibata et al. 2019). A large fraction of these old and metal-poor structures are observed as narrow and 1D structures (Grillmair & Carlin 2016), and are explained as stellar debris produced from globular clusters (GCs) that were perhaps brought in by their parent dark satellite galaxies during accretion (Renaud et al. 2017). Due mainly to their simple morphology and lack of associations with any other observed components of the stellar halo, the GC streams are generally modeled independently as simple GCs disrupting under the tidal force field of the host galaxy (e.g., Dehnen et al. 2004). In effect, the good match between observations and such simple models also favors primeval models of GC formation—a scenario in which GCs originate from dark matter free gravitationally bound gas clouds in the early universe (Kravtsov & Gnedin 2005; Kruijssen 2014), and then later migrate into the host galaxy.

In this work, we report the discovery of a new Milky Way stream, and find that it criss-crosses through the previously well known "GD-1" stream. We demonstrate that GD-1 and this new structure are highly correlated in distance and kinematics, and have similar stellar populations. We discuss the possible interpretations of the origin of this remarkable entangled system, and the potential implications of our results in dark matter and GC formation studies.
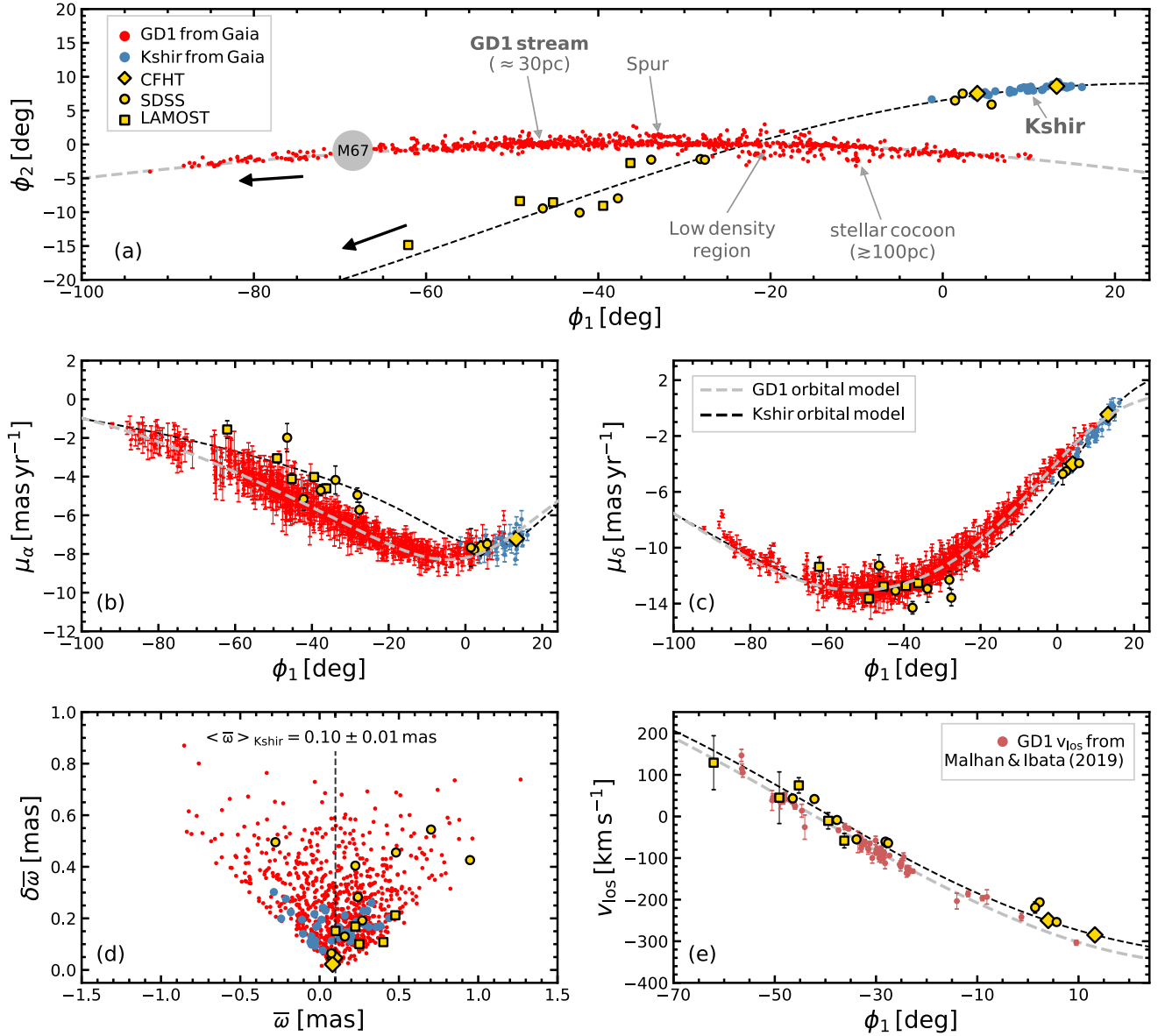
2. GD-1 and Its Neighbor

Ranging in heliocentric distance between $d_\odot \sim 8–12$ kpc, the GD-1 stream (Grillmair & Dionatos 2006) has been observed as an $\sim 80°$ long (~ 12 kpc, Price-Whelan & Bonaca 2018), narrow (≈ 20 pc in physical width, Koposov et al. 2010), linear stellar structure. This GC stream is dynamically very cold (with a velocity dispersion of ≈ 1 km s^{-1}, Malhan & Ibata 2019, MI19 hereafter) and is remarkably metal deficient ([Fe/H] $= -2.24 \pm 0.21$ dex).

Figure 1(a) shows the density map in the region around GD-1 that we obtained by processing the entire European Space Agency (ESA)/*Gaia* data release 2 (DR2) data set (Gaia Collaboration et al. 2018; Lindegren et al. 2018) with the STREAMFINDER software (Malhan & Ibata 2018; Malhan et al. 2018; Ibata et al. 2019). Briefly, STREAMFINDER works by examining every star in the *Gaia* survey in turn, sampling the possible orbits consistent with the observed photometry and kinematics, and finding the maximum-likelihood stream solution given a contamination model and a stream model. As in Malhan et al. (2018), we de-reddened the survey using the Schlegel et al. (1998) dust maps, and kept only those stars with (de-reddened) $G_0 < 19.5$ to ensure homogeneous depth over the sky. The stream width parameter in the search algorithm was set to 50 pc, and we used single stellar population (SSP) template models from the PARSEC stellar tracks library (Bressan et al. 2012) of age 12.5 Gyr, and scanned a range of metallicities of [Fe/H] $= -2.2$, -2.0, -1.6, -1.2, -0.8, -0.4. For each processed star, we thus obtained six stream solutions, corresponding to the six trial SSP metallicity values, and we accepted the solution that yielded the highest likelihood. GD-1 appears as a completely distinguished structure in our STREAMFINDER maps, as shown in Figure 1(a). It transpires that the best orbital solution for 88% of the GD-1 stars is obtained with an SSP template with metallicity [Fe/H] $= -2.2$, similar to the measured [Fe/H] value (MI19).[5]

---

[5] The value 88% corresponds to the fraction of stars (identified as GD-1) obtained as stream solution using that particular [Fe/H] model.

Figure 1. Spatial and kinematic distribution of GD-1 and Kshir. (a) Sky position in $\phi_1 - \phi_2$ coordinates, which are a rotated celestial system aligned along GD-1. The narrow GD-1 ($\approx$30 pc wide) can be immediately spotted along $\phi_2 \sim 0°$. Some additional features can also be observed, such as the low density regions along the stream, the "spur" component and the "cocoon" component ($\gtrsim$100 pc wide). An arc-like structure can be seen at $(\phi_1, \phi_2) \sim (10°, 8°)$, which we refer to as "Kshir." Spectroscopically confirmed members for Kshir are shown in yellow. The region of sky containing the foreground open cluster M67 ($d_\odot \sim 0.9$ kpc) was masked out prior to the running of the STREAMFINDER. The bold arrows indicate the direction of motion of the two streams. Panels (b)–(d) show, respectively, proper motion in μ_α, μ_δ, and parallax $\overline{\omega}$, as a function of ϕ_1. Panel (e) shows the heliocentric line-of-sight (LOS) velocities v_{los} of the members of GD-1 (pink) and Kshir (yellow). The derived orbits of the two structures are shown in each panel, and can be seen to be very similar.

We also set the stream-detection significance to $>8\sigma$, which means that at the position of every star, the algorithm finds that there is a $>8\sigma$ significance for there to be a stream-like structure. This results in a sample of 811 stars in the region around GD-1 that are shown in Figure 1(a) (red and blue points). The region of the sky containing the foreground open cluster M67 was masked out prior to running the STREAMFINDER.

Figure 1(a) reveals the complex structure that surrounds the thin GD-1 stream (shown with red points). The plot is presented in $\phi_1 - \phi_2$ coordinates (Koposov et al. 2010), which align along GD-1. A narrow component of GD-1 ($\approx$30 pc wide) can be readily seen along $\phi_2 \approx 0°$, enveloped by a broad and diffuse structure ($\gtrsim$100 pc wide). This extended component was previously reported in Malhan et al. (2019), and was referred to as the *cocoon* component. The code also tentatively

detected the previously known low density regions and the "spur" component (Price-Whelan & Bonaca 2018).

The present study focuses on the detection of the arc-like feature that is conspicuously visible in Figure 1(a) at $(\phi_1, \phi_2) \approx (10°, 8°)$, skirting almost parallel to GD-1 (shown with blue points). We refer to this structure as "Kshir."[6] Based on the orbital analysis of the STREAMFINDER code, we note that both Kshir and GD-1 are found by the algorithm with similar values of the z-component of angular momentum (L_z) and energy (E). In particular, the algorithm (in the adopted potential model) estimates $(L_z, E)_{\rm GD1} = (2900 \pm 800 \text{ kpc km s}^{-1}, -88{,}000 \pm 19{,}000 \text{ km}^2 \text{ s}^{-2})$ and $(L_z, E)_{\rm Kshir} = (3200 \pm 600 \text{ kpc km s}^{-1}, -89{,}000 \pm 13{,}000 \text{ km}^2 \text{ s}^{-2})$. This indicates that they are,

---

[6] In Hindu mythology, Kshir refers to an ocean of milk.

Table 1
Spectroscopically Confirmed Members of Kshir

R.A. J2000 (deg)	Decl. J2000 (deg)	v_{los} (km s^{-1})	[Fe/H] (dex)	Source
201.53579	67.28841	−206.32	−1.78	S
205.87918	67.57526	−249.95	…	C
230.38107	68.16672	−284.78	…	C
147.96434	9.65499	129.28	−1.56	L
150.32399	23.73448	45.09	−1.76	L
153.05409	25.1087	43.33	−1.74	S
153.10830	26.59341	74.75	−1.41	L
154.73641	37.16519	−58.23	−1.47	L
156.31086	39.28787	−54.95	−1.94	S
156.64035	27.9157	41.96	−1.71	S
157.84587	30.59822	−10.42	−2.1	L
158.26272	32.5852	−8.47	−1.67	S
161.53675	43.45613	−60.52	−2.13	S
162.14438	43.73839	−64.03	−1.99	S
199.92916	66.09159	−218.86	…	S
210.43905	66.11245	−253.76	−1.83	S

Note. The sky coordinates are from *Gaia* DR2, while the v_{los} and [Fe/H] are measurements from CFHT (C), SEGUE (S), and Large Sky Area Multi-Object Fibre Spectroscopic Telescope (LAMOST) (L).

perhaps, part of the same coherent group and share a common origin. The STREAMFINDER detects a total of 42 stars for the Kshir stream from *Gaia* DR2. We realized that one of these stars fortuitously had a spectroscopic observation in the Sloan Digital Sky Survey (SDSS)/Segue (DR10; Yanny et al. 2009), from which we obtained the metallicity ([Fe/H]) and line-of-sight (LOS) velocity (v_{los}) values. A further two stars were observed with the ESPaDOnS high-resolution spectrograph on the Canada–France–Hawaii Telescope (CFHT) in service mode, as a part of our own follow up program. The data were reduced with the Libre-ESpRIT pipeline (Donati et al. 1997), and we measured the stars' velocities using the fxcor command in IRAF. The chemical abundances of the stars (which are part of a much larger sample of streams) are currently being analyzed, and will be presented in a later contribution. These three stars are mentioned in the top rows of Table 1 and are also shown in Figure 1. Kshir is already visible in Figure 1 of Malhan et al. (2019); however, it was not focused upon as we previously lacked spectroscopic measurements for this structure.

We used the Kshir orbit model, derived in Section 3, to find additional member stars that lie along its trajectory. To this end, we used the 5D astrometric measurements (that came from *Gaia* DR2 for blue stars shown in Figure 1(a)), in combination with the aforementioned three velocity measurements, for Kshir stars to obtain a solution for its orbit. This orbit-fitting procedure is detailed in Section 3. We now assume that we possess a reasonable orbital representation of the Kshir structure.

To identify additional spectroscopic members of Kshir, we first created a special data set by cross-matching the *Gaia* DR2 catalog with the SDSS (Yanny et al. 2009) and LAMOST data release 4 (DR4; Zhao et al. 2012) spectroscopic data sets, and selected those stars with *Gaia* colors in the range $(0.40 < [G_{BP} − G_{RP}]_0 < 1.60)$, with magnitude ($G_0 < 20$), and with spectroscopic metallicity [Fe/H] < −0.5 dex. We further selected those stars that lie within 3σ of Kshir's orbit
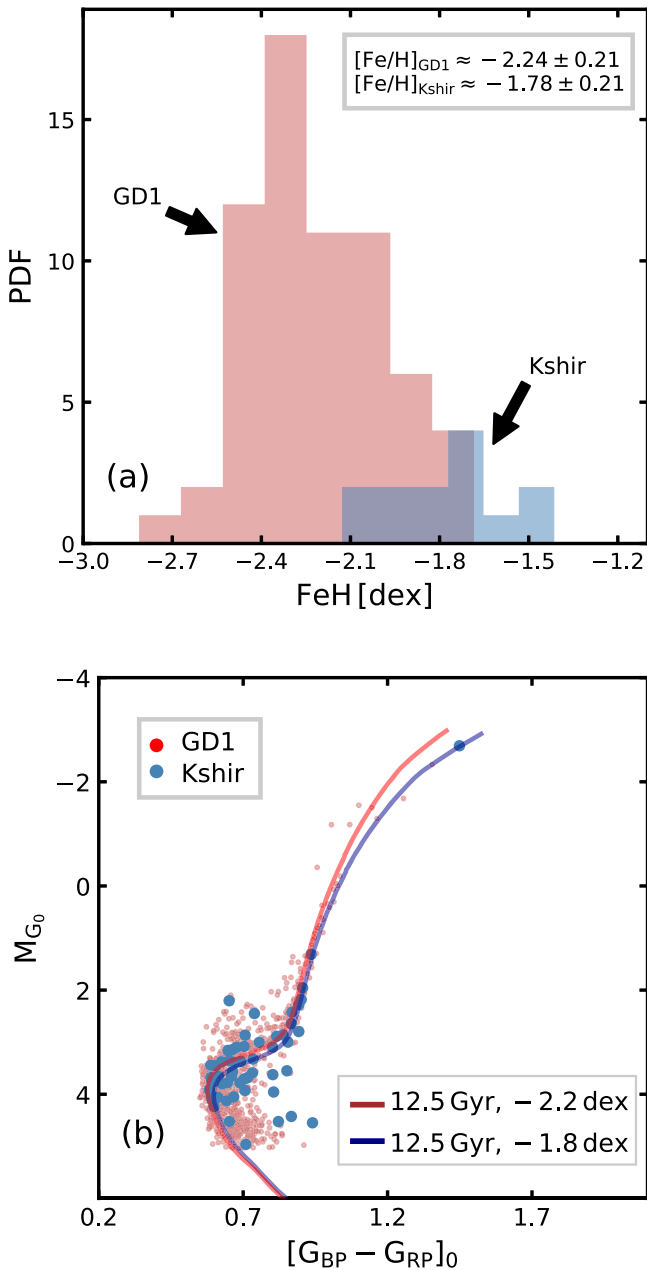
model in the observed parallax (ϖ), proper motion (μ_α, μ_δ), and LOS velocity v_{los} space, and within ∼300 pc perpendicular to the orbit (which defines the maximum possible stream width). We do not make any additional selections in photometry and [Fe/H] at this stage, since we do not a-priori know the properties of Kshir's stellar population. This 6D selection yields a total of 13 stars (eight from SEGUE and five from LAMOST), that represent additional Kshir's candidate members. These stars were not previously identified by the STREAMFINDER due to their lower contrast. We verified that the expected contamination from a smooth halo model (as predicted by the GUMS simulation; Robin et al. 2012) along Kshir's orbit is nearly zero.

The combined phase-space properties of the stellar members of Kshir and GD-1 are plotted in Figures 1(a)–(e) (along with the spectroscopically confirmed members for Kshir that are shown in yellow). One readily observes that GD-1 and Kshir intersect spatially, at $\phi_1 \approx −20°$, and are also strongly entangled in proper motion space. In the v_{los} panel, the stars corresponding to GD-1 refer to the spectroscopically confirmed members inventoried in MI19. It can be easily discerned that Kshir stars lie quite close to the GD-1 stars even in v_{los} space. The orbit of GD-1 (obtained from MI19) and Kshir look very similar in every phase-space dimension, and Kshir's orbit predicts similar v_{los} gradient along the length of the stream as observed for GD-1, with an almost constant offset of ≈20 km s^{-1}. We caution that the lack of stars between ∼−25° and 0° in Kshir may either be physical in origin, or could be due to the selection effect of the SEGUE and LAMOST surveys; however, it is hard to quantify at this stage. Also note that the leading part of Kshir (dominated by 6D members) appears much wider than the trailing part. This result could be specific to the criteria adopted here to select Kshir stars, and future analysis (with a larger sample size) should better characterize the structural morphology of this stream.

The uncertainty-weighted average mean parallax for Kshir (for blue points in Figure 1) is $\langle\overline{\varpi}\rangle = 0.10 \pm 0.01$ mas, i.e., ∼10 kpc in distance, which is similar to the distance of the GD-1 orbit in the same range of ϕ_1 (∼8.5 kpc). The metallicities of Kshir and GD-1 are compared in Figure 2(a). We find [Fe/H] = $−1.78 \pm 0.21$ dex for Kshir, implying that it is systematically more metal-rich than GD-1 by ∼0.4 dex. On performing a two-sample Kolmogorov–Smirnov (KS) test for the null hypothesis that the two [Fe/H] samples are drawn from the same distribution, the resulting probability was found to be $p_{KS} = 3.78 \times 10^{-5}$: indicating that the hypothesis can be rejected at the 4σ level. Their stellar populations are compared in Figure 2(b), where we display the magnitudes corrected for the distance of the stars, as estimated from the orbit models at the corresponding value of ϕ_1. While the color–magnitude diagrams appear similar, the metallicity distributions suggest that the stellar populations are not identical.

3. Orbit

In MI19 we implemented an orbit-fitting procedure to a sample of GD-1 stars in order to constrain the gravitational potential of the Milky Way. This orbit is shown in Figure 1. Here we fix the Galactic potential model derived in that study (which has a circular velocity at the Solar radius of $V_{circ}(R_\odot) = 244$ km s^{-1}, and a density flattening of the dark halo as $q_\rho = 0.82$), and follow a similar procedure (with

Figure 2. Metallicity and photometry of GD-1 and Kshir. Top panel: [Fe/H] distribution of spectroscopically confirmed members of GD-1 (red) and Kshir (blue) stars. Bottom panel: *Gaia* (de-reddened) color–magnitude diagram of all member stars of Kshir and GD-1, previously shown in Figure 1. The absolute magnitude were then obtained by correcting the observed magnitude value for the orbital distance of each star. Two SSP template models, corresponding to the mean metallicity values of the streams, are also shown.

identical likelihood function) as that presented in MI19 to fit the orbit of Kshir.

We used the 42 Kshir stars identified by the STREAMFINDER (shown as blue points in Figure 1), in combination with the three velocity measurements from CFHT and SEGUE that are available for those targets.[7] The best-fit orbit for Kshir is shown in

---

Figure 1. We find its orbit to be more circular than that of GD-1 (see Figure 3), but with L_z ($\sim2700 \pm 200$ kpc km s^{-1}) comparable to that of GD-1 ($L_z \sim 2950$ kpc km s^{-1}, MI19). The difference in the L_z values stems from the aforementioned offset in the kinematic measurements between the two structures.

These orbits suggest that the last closest approach between Kshir and GD-1 occurred ~1.7 Gyr ago with an impact parameter of ~1–2 kpc, although we caution that these values depend on the assumed Galactic potential model.

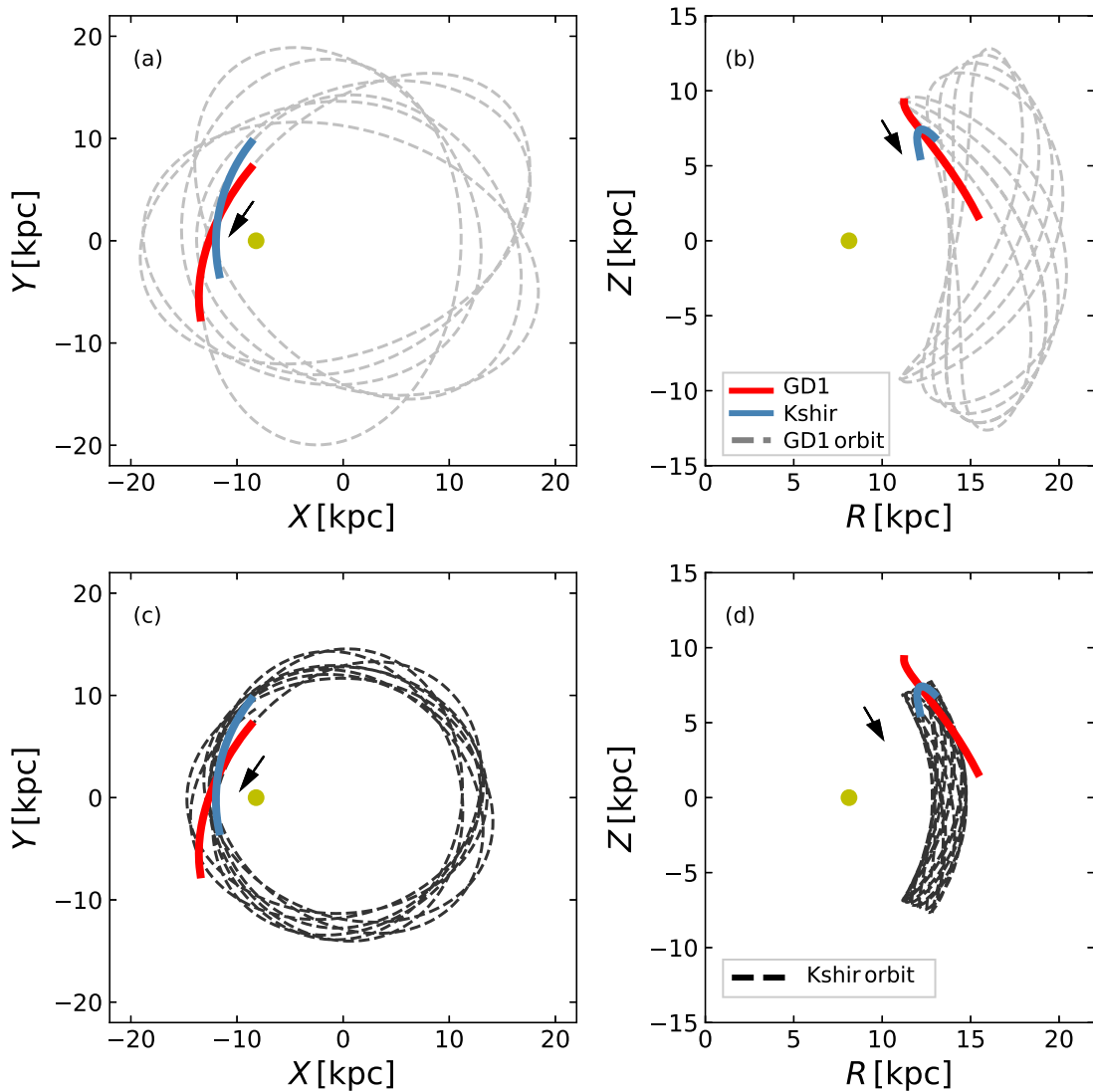## 4. Discussion and Conclusions

We have presented the discovery of a new stream structure, referred to as "Kshir," which criss-crosses the well-studied GD-1 stream on the sky, lies at similar distance, and possesses very similar kinematics (Figure 1). Moreover, we find Kshir to be also an old and metal-poor structure ([Fe/H] $\approx -1.78 \pm 0.21$ dex), though slightly more metal-rich than GD-1 (Figure 2). Figure 1(a) shows that Kshir's orbit intersects GD-1 at $\phi_1 \sim -20°$, which is also the location of the tentative "gap" present along GD-1 (Price-Whelan & Bonaca 2018).

Such a phase-space entanglement in GC streams has not previously been reported. This makes the nature and origin of Kshir, and its possible association with GD-1, very intriguing. We consider below three explanations for the observed correlation.

(A) Orbital wraps of same structure. If Kshir and GD-1 stemmed from the same GC progenitor, then the observed configuration could be due to the presence of different orbital wraps. In this case, Kshir might possibly be a portion of the GD-1 stream that is wrapped by $\sim360°$ (or multiples thereof). The fact that Kshir does not simply line up along the orbit of GD-1 (Figure 3) argues against this possibility, although we stress that this result is valid only for the adopted potential derived in MI19. It is possible that other, more complex, Galactic potentials could simultaneously fit extant data and allow Kshir to be a simple wrap of GD-1. Nevertheless, this scenario seems unlikely, due to the difference in the chemical composition of the two structures. This consideration does not completely rule out the scenario, however, since it is possible that the progenitor satellite may have possessed a radial metallicity gradient (like, e.g., ω Cen, Johnson & Pilachowski 2010). If tides act slowly, they disrupt the progenitor by progressively removing its outskirts, which can then result in the tidal stream possessing metallicity variations along its length.

(B) A chance alignment of two independent GCs. It is possible that Kshir and GD-1 are tidal debris of two unassociated GCs. However, given the vast phase-space volume of the Milky Way, such a degree of phase-space overlapping of two unrelated stellar substructures is a low likelihood event. To obtain an estimate of the corresponding probability, we implemented the following test. Employing the HaloTools package (Hearin et al. 2017), we randomly generated a phase-space distribution in an isotropic Navarro–Frenk–White (NFW) halo profile (Navarro et al. 1996), with a virial mass of $1.28 \times 10^{12} M_\odot$ (Watkins et al. 2019). From this distribution we calculated the probability that two randomly drawn tracer particles at the distance of the objects of interest have similar orbits. Concretely, we drew 10^4 random pairs of particles in the Galactocentric distance range between 13 and 15 kpc and counted the number of times these pairs possessed

Figure 3. Orbital trajectories of GD-1 and Kshir in the Galactocentric Cartesian system. Top panels: GD-1's orbit (silver). For perspective, the current locations of GD-1 (red) and Kshir (blue) are also shown. The Galactic center lies at the origin and the Sun (yellow dot) is at (X, Y, Z) = (−8.122, 0, 0) kpc. The orbit was integrated backwards in time for 3 Gyr. The arrows represent the direction of motion of the structures. Bottom panels: as above, but showing Kshir's orbit (black).

a relative difference in the *z*-component of angular momentum of $\Delta L_z < 300$ kpc km s^{-1}, and with relative difference in the energy per unit mass of $\Delta E < 10,000$ km^2 s^{-2} (as is the case of Khsir and GD-1). We found this probability to be ∼0.007. This implies that if Kshir and GD-1 are unrelated, then the probability of their chance phase-space alignment is <1%.

(C) Common origin. The degree of phase-space correlation as we observe for Kshir and GD-1 is possible if the two structures originated from a common parent sub-halo that was accreted onto the Milky Way. Under this scenario, the stellar contents of the sub-halo system would be deposited on very similar orbits. Cosmological simulations show that GCs that evolve within their dark sub-halos, and later accrete into the host halo, give rise to stellar streams that possess substantial morphological complexity (Carlberg 2018a). This often results in secondary stellar components that accompany the primary GC stream track (see figures in Carlberg 2018b), with the overall structure remaining kinematically coherent (much like we see here for Kshir and GD-1). In addition to this, the cosmological simulations further show that the accreted GC streams should lie embedded in broader and dispersed star

streams. The reason for this is that the primary stream (which is thin and dense) that survives to the present day is formed once the GC escapes the parent sub-halo and is deposited into the main halo, whereas the wider stellar component enveloping the thin stream is the relic of the stars that were continually removed from the GC while it remained in its parent dark sub-halo. Evidence for this broader stream in GD-1 (labeled "cocoon" in Figure 1(a)) was already reported in Malhan et al. (2019). Moreover, these simulations also show criss-crossing of streams from separate GCs that formed in a single sub-halo; although an implication is that the sub-halo must be sufficiently massive to host multiple GCs. Therefore, both the Kshir structure and the existence of "cocoon" in the neighborhood of GD-1 strengthen the case for this "accretion" scenario. Further, the measured difference in metallicity between the two structures argues against a single GC progenitor, although again the constraint is not entirely conclusive (partially because the progenitor could have possessed a radial metallicity gradient). Alternatively, GD-1 and Kshir may correspond to stellar debris produced from either different GC members of the same dark sub-halo, or Kshir may perhaps be debris of the

stellar component of the dwarf galaxy that was stripped off during the accretion. A detailed chemical abundance analysis will help to distinguish between these possibilities. Assuming the hypothesized dwarf galaxy hosted a metal-poor GC and a field population with $[Fe/H]_{field} \sim -1.78$ dex, we estimate its total stellar mass as $M_* \sim 10^5 M_\odot$ (using the stellar mass–stellar metallicity relation from Kirby et al. 2013), implying $M_{halo} \sim 10^{8-9} M_\odot$ (from stellar-to-halo-mass relation from Read et al. 2017). This makes the progenitor very similar to Eridanus II dwarf (Bechtol et al. 2015), which is also known to host a single GC (Crnojević et al. 2016). However, if the dwarf hosted two GCs (and assuming the field stars to be at least as metal-rich as the GCs), then the above quoted mass values in this case would represent typical lower bounds. None of the luminous satellites have orbits close to GD-1's trajectory (Bonaca et al. 2019b); however, a future detection of a faint disrupting galaxy along GD-1's/Kshir's orbit would serve as "smoking gun" evidence for the proposed accretion scenario. On the other hand, its lacks supports a scenario where Kshir and GD-1 were perhaps accreted as GC(s) within an empty dark sub-halo.

The stellar streams of the Milky Way have unexpectedly revealed their rather complex morphologies (Price-Whelan & Bonaca 2018; Bonaca et al. 2019a; Malhan et al. 2019), which presents evidence for a formation mechanism that appears incompatible with a simple tidal disruption model. Modeling GD-1, particularly in light of these new observational constraints, may allow us to develop an understanding of the origins of these recently found complexities in this well-studied system. This may also allow us to examine whether some GCs can form in otherwise empty cold dark matter sub-halos before, or shortly after re-ionization began (e.g., Peebles 1984; Mashchenko & Sills 2005; Ricotti et al. 2016), giving rise to stream structures that exhibit multiple structural components. A detailed dynamical and chemical analysis of GD-1 and Kshir may potentially be useful in distinguishing in situ and accreted GC stream, and in probing the initial conditions of the dark sub-halo within which they came.

ORCID iDs

Khyati Malhan ⓘ https://orcid.org/0000-0002-8318-433X
Rodrigo A. Ibata ⓘ https://orcid.org/0000-0002-3292-9709
Raymond G. Carlberg ⓘ https://orcid.org/0000-0002-7667-0081
Michele Bellazzini ⓘ https://orcid.org/0000-0001-8200-810X
Benoit Famaey ⓘ https://orcid.org/0000-0003-3180-9825
Nicolas F. Martin ⓘ https://orcid.org/0000-0002-1349-202X

References

Balbinot, E., Yanny, B., Li, T. S., et al. 2016, ApJ, 820, 58
Bechtol, K., Drlica-Wagner, A., Balbinot, E., et al. 2015, ApJ, 807, 50
Belokurov, V., Zucker, D. B., Evans, N. W., et al. 2006, ApJL, 642, L137
Bernard, E. J., Ferguson, A. M. N., Schlafly, E. F., et al. 2016, MNRAS, 463, 1759
Bonaca, A., Conroy, C., Price-Whelan, A. M., & Hogg, D. W. 2019a, ApJL, 881, L37
Bonaca, A., Hogg, D. W., Price-Whelan, A. M., & Conroy, C. 2019b, ApJ, 880, 38
Bressan, A., Marigo, P., Girardi, L., et al. 2012, MNRAS, 427, 127
Carlberg, R. G. 2018a, ApJ, 861, 69
Carlberg, R. G. 2018b, arXiv:1811.10084
Crnojević, D., Sand, D. J., Zaritsky, D., et al. 2016, ApJL, 824, L14
Dehnen, W., Odenkirchen, M., Grebel, E. K., & Rix, H.-W. 2004, AJ, 127, 2753
Donati, J.-F., Semel, M., Carter, B. D., Rees, D. E., & Collier Cameron, A. 1997, MNRAS, 291, 658
Gaia Collaboration, Brown, A. G. A., Vallenari, A., et al. 2018, A&A, 616, A1
Grillmair, C. J. 2009, ApJ, 693, 1118
Grillmair, C. J., & Carlin, J. L. 2016, in Tidal Streams in the Local Group and Beyond, ed. H. J. Newberg & J. L. Carlin (Cham: Springer), 87
Grillmair, C. J., & Dionatos, O. 2006, ApJL, 643, L17
Hearin, A. P., Campbell, D., Tollerud, E., et al. 2017, AJ, 154, 190
Ibata, R., Irwin, M., Lewis, G. F., & Stolte, A. 2001, ApJL, 547, L133
Ibata, R. A., Malhan, K., & Martin, N. F. 2019, ApJ, 872, 152
Johnson, C. I., & Pilachowski, C. A. 2010, ApJ, 722, 1373
Kirby, E. N., Cohen, J. G., Guhathakurta, P., et al. 2013, ApJ, 779, 102
Koposov, S. E., Rix, H.-W., & Hogg, D. W. 2010, ApJ, 712, 260
Kravtsov, A. V., & Gnedin, O. Y. 2005, ApJ, 623, 650
Kruijssen, J. M. D. 2014, CQGra, 31, 244006
Lindegren, L., Hernandez, J., Bombrun, A., et al. 2018, A&A, 616, A2
Malhan, K., & Ibata, R. A. 2018, MNRAS, 477, 4063

Malhan, K., & Ibata, R. A. 2019, MNRAS, 486, 2995
Malhan, K., Ibata, R. A., Carlberg, R. G., Valluri, M., & Freese, K. 2019, ApJ, 881, 106
Malhan, K., Ibata, R. A., & Martin, N. F. 2018, MNRAS, 481, 3442
Mashchenko, S., & Sills, A. 2005, ApJ, 619, 243
Myeong, G. C., Jerjen, H., Mackey, D., & Da Costa, G. S. 2017, ApJL, 840, L25
Navarro, J. F., Frenk, C. S., & White, S. D. M. 1996, ApJ, 462, 563
Peebles, P. J. E. 1984, ApJ, 277, 470
Price-Whelan, A. M., & Bonaca, A. 2018, ApJL, 863, L20
Read, J. I., Iorio, G., Agertz, O., & Fraternali, F. 2017, MNRAS, 467, 2019
Renaud, F., Agertz, O., & Gieles, M. 2017, MNRAS, 465, 3622
Ricotti, M., Parry, O. H., & Gnedin, N. Y. 2016, ApJ, 831, 204
Robin, A. C., Luri, X., Reylé, C., et al. 2012, A&A, 543, A100
Schlegel, D. J., Finkbeiner, D. P., & Davis, M. 1998, ApJ, 500, 525
Shipp, N., Drlica-Wagner, A., Balbinot, E., et al. 2018, ApJ, 862, 114
Watkins, L. L., van der Marel, R. P., Sohn, S. T., & Evans, N. W. 2019, ApJ, 873, 118
Yanny, B., Rockosi, C., Newberg, H. J., et al. 2009, AJ, 137, 4377
Zhao, G., Zhao, Y., Chu, Y., Jing, Y., & Deng, L. 2012, arXiv:1206.3569